https://doi.org/10.5194/cp-2020-93
Preprint. Discussion started: 10 August 2020

Climate of the Past Discussions

The response of annual minimum temperature on the eastern central Tibetan Plateau to large volcanic eruptions for the period 1380–2014 AD

Yajun Wang[1], Xuemei Shao[1,2], Yong Zhang[1], Mingqi Li[1]

[1] Key Laboratory of Land Surface Pattern and Simulation, Institute of Geographic Sciences and Natural Resources, Chinese Academy of Sciences (CAS), Beijing, 100101, China
[2] University of Chinese Academy of Sciences, Beijing, 100049, China

Correspondence to: Yong Zhang (zhangyong@igsnrr.ac.cn)

Abstract. Volcanic eruptions have a significant impact on global temperature; their consequences are of particular interest in regions that are especially sensitive to climate change, like the Tibetan Plateau. In this study, we develop a temperature-sensitive tree-ring width standard chronology covering the period 1348–2014 AD using Qilian juniper (*Sabina przewalskii* Kom.) samples collected from Animaqin Mountain on the Tibetan Plateau. We reconstruct the annual (prior August to current July) mean minimum temperature (T_{min}) since 1380 AD and show that our reconstruction explains 58% of the variance during the 1960-2014 calibration period. Our results demonstrate in 77.8% of cases in which a volcanic eruption with a volcanic explosivity index of 5 or greater occurs, temperature decreases in the year of or the year following the eruption. The results of the Superposed Epoch Analysis also indicate that there is a high probability that the T_{min} decreases within 2 years of a large volcanic eruption, especially when such eruptions occur in low latitudes.

Keywords. Tibetan Plateau, tree rings, minimum temperature, volcanic eruption

1 Introduction

Large volcanic eruptions can affect the climate of the Earth (Robock, 2000) and have played a major role in past global temperature changes (Salzer and Hughes, 2007). Eruptions pour large amounts of ash particles and gases into the atmosphere, much of which are carried to other regions by atmospheric movement. These materials efficiently reflect incident solar radiation, resulting in the cooling of the Earth's surface. However, volcanic eruptions of similar magnitudes do not necessarily result in cooling across all areas of the world. For example, the 1991 eruption of Mount Pinatubo, Philippines, caused summer cooling over much of the globe in 1992, but the temperature in some areas was above average (Robock and Mao, 1992). Thus, it is not necessarily clear to what extent or in what manner a strong volcanic eruption will influence temperature in a particular region.

https://doi.org/10.5194/cp-2020-93
Preprint. Discussion started: 10 August 2020

Climate of the Past
Discussions

Often referred to as the "third pole", the Tibetan Plateau (TP) is especially sensitive to climate change (Yao et al., 2012) and may therefore be more profoundly influenced by volcanic eruptions. Jia and Shi (2001) studied climate signals following volcanic eruptions from 1950 to 1997 and found that temperature on the TP dropped within 2 years after significant eruptions during this period. Zhang and Zhang (1985) analyzed the relationship between large volcanic eruptions and temperature changes from 1951 to 1985 in northwestern China and found that temperature minimums appeared 8, 15, and 18 months after eruptions; they also found temperature maximums 6 months after eruptions. These studies show that temperature on the TP is affected by volcanic activities, but it is important to note that they are based on instrumental data, which covers a relatively short time span. Temperature changes caused by strong volcanic eruptions can affect tree growth (Tognetti et al., 2012), an influence that can be seen in the rings of certain trees (D'Arrigo et al., 2013; Filion et al., 1986; Lamarche and Hirschboeck, 1984) and used to identify past volcanic activity (D'Arrigo et al., 2013; Filion et al., 1986; Lamarche and Hirschboeck, 1984). Especially when long-lived trees are available, tree-rings can serve as temperature-sensitive proxies for investigating climate responses to volcanic eruptions that occurred prior to the instrumental record (D'Arrigo et al., 2013; Salzer and Hughes, 2007).

Tree rings from the TP can potentially be used to study the climate response to volcanic activities. Previous tree-ring based researches showed that some cold years can be closely correlated with large volcanic events (Liang et al., 2008; Liang et al., 2016; Zhang et al., 2014). Li et al (2017) quantitatively assessed the correlation between temperature changes in the southeastern TP and volcanic eruptions and showed that most of the years of extreme cold in the past 304 years occurred 1–2 years after major volcanic eruptions. However, the influence of volcanic eruptions on temperatures on the TP over the long-term is less well understood due to the paucity of data in this region.

the Animaqin Mountains are located on the northeastern TP, many long tree-ring series, with hundreds of years or even thousands of years (Chen et al., 2016; Gou et al., 2007; Gou et al., 2008; Gou et al., 2010), were developed here, and provided a significant proxy for the tree growth response to volcanic dynamics, but the response studying of tree rings to volcanic activity is still rare across this area even the TP. Using tree-ring samples of Qilian juniper (*Sabina przewalskii* Kom.) collected from the Animaqin Mountains, this study develops a 667-year tree-ring width chronology that is used to reconstruct annual mean minimum temperatures (T_{min}) across the east-central TP. This chronology is then used to explore the response of T_{min} to strong volcanic eruptions over the past six centuries.

https://doi.org/10.5194/cp-2020-93
Preprint. Discussion started: 10 August 2020

Climate of the Past Discussions

2 Data and methods

2.1 Tree-ring data

Qilian juniper samples were taken at Ningmute Forest Farm(NMT), Henan County, Qinghai Province, China. This area is located in the sub-frigid zone and has a semi-humid climate (Zheng et al., 2013) in which precipitation is mainly concentrated between May and September. Because the site is close to the Yellow River and the soil layer in the forest area is thick, the moisture conditions of the forest are good. The regional vegetation zone is coniferous forest and the main tree species include *Sabina przewalskii Kom.*, *Picea* crassifolia Kom., *Betula spp.*, *Salix cheilophila*, and others. The study area is located on the southern slope of the Animaqin Mountains and ranges in elevation from 3523 to 3900 m a.s.l. (Figure 1). The gradient of the slope is 30°–40°. A total of 110 cores from 55 trees were drilled at breast height with an increment borer in 2015.

(figure 1 near here)

The cores were air-dried, fixed to wooden mounts, polished, and cross-dated. The cores were then measured using a Lintab 6 tree-ring width measuring instrument with a resolution of 0.01 mm. The COFECHA program (Holmes, 1983) was used to check the quality of the cross-dating and the accuracy of the measurements. The signal-free (SF) standardization method (Melvin and Briffa, 2008) was adopted to standardize the tree-ring data in order to minimize trend distortion in the chronologies produced by the straight-line detrending method. The RCSigFree program (https://www.ldeo.columbia.edu/tree-ring-laboratory/resources/software) was used to establish the tree-ring width chronology. In this procedure, the age trend curve was fitted to cubic smoothing splines with a 50% cutoff at approximately 67% of the mean segment length. The validity of the SF chronology was assessed using the mean correlation coefficient for the tree-ring series (Rbar) and the value of the expressed population signal (EPS).

2.2 Instrumental data

Thirteen meteorological stations in the region of the sampling site were identified: Zhongxinzhan (ZXZ), Dari (DR), Xinghai (XH), Guoluo (GL), Tongde (TD), Guinan (GN), Zeku (ZK), Henan (HN), Jiuzhi (JZ), Tongren (TR), Maqu (MQ), Langmusi (LMS), and Hezuo (HZ). For each station, data for four climate parameters – monthly total precipitation (P), monthly mean temperature (T_{mean}), monthly mean minimum temperature (T_{min}), and monthly mean maximum temperature (T_{max}) – were extracted from the China Meteorological Data Sharing Service System (http://www.cma.gov.cn/2011qxfw/2011qsjgx). Details are provided in Table 1.

(Table 1 near here)

https://doi.org/10.5194/cp-2020-93
Preprint. Discussion started: 10 August 2020

Because the observation intervals of the stations shown in Table 1 differ, it was necessary to select the longest record to ensure the stability of the correlation function. Seven stations with instrumental data for < 30 years were excluded firstly: GL, GN, and TR (all of which were established in the 1990s), and ZXZ, TD, ZK, and LMS (all of which ceased in the 1980s or 90s). Climate data from the other six stations (DR, XH, HN, JZ, MQ, and HZ) were used for the following analysis. In the quality control of instrumental data of the six stations, we found that there are some problems in the instrumental data of HN station, and then corresponding processing was carried out. The detailed relevant information is listed in the supplementary section. Finally, taking the means for the interval 1971–2000 as the references, the precipitation departure percentages and temperature departures were calculated and averaged for all six stations. The mean values calculated in this way were then considered to be representative of the regional climate. The monthly climate data from the previous July to the current September were used to analyze the response of tree growth to climate change.

2.3 Volcanic data

Data about volcanic activity were obtained from the Volcanic Explosivity Index (VEI) sequence published by the Smithsonian Institution Global Volcanism Program (http://volcano.si.edu). Globally, there have been 46 strong volcanic eruptions (VEI ≥ 5) since 1380 AD. For this study, it is important to note that eruptions that occurred in October, November, or December of a given year are marked as being a volcanic event in the following year. This is because tree radial growth mostly stops in October on the TP. We developed 7 sets of volcanic data for further analysis based on geography: (a) global; (b) Northern Hemisphere; (c) Southern Hemisphere; (d) low latitude 30°S–30°N; (e) Northern Hemisphere mid-latitude 30°N–60°N ; (f) Southern Hemisphere mid-latitude 30°S–60°S; and (g) Northern Hemisphere high latitude.

2.4 Methods

The correlation function was used to analyze the relationship between the tree-ring width index and climatic factors. The fitted equation was then established using a simple linear regression and verified by the cross-validation method (Michaelsen, 1987) and split-period calibration/verification analysis (Meko and Graybill, 1995). Several statistical tests (sign test, product mean value, reduction error, and coefficient of efficiency) were utilized. The split periods for calibration were 1960–1991 and 1984–2014. The correlations between the observed and reconstructed series and the gridded dataset (TS3.22; Mitchell and Jones, 2005) from the University of East Anglia Climatic Research Unit (CRU) were analyzed using the KNMI Climate Explorer research tool (http://climexp.knmi.nl). The

https://doi.org/10.5194/cp-2020-93
Preprint. Discussion started: 10 August 2020

Climate of the Past
Discussions

Superposed Epoch Analysis (SEA) method (Brad et al., 2003; Singh and Badruddin, 2006) was also used to assess quantitatively the impact of volcanic eruption on temperature in the east-central TP.

3 Results

3.1 Statistical characteristics of the chronology

The tree-ring width chronology covers the time period from 1348 to 2014 AD (Figure 2a), with an average length of 325.1 years. The average sensitivity is 0.171; and the first-order autocorrelation coefficient is 0.261. The signal-to-noise ratio is 21.870, the EPS is 0.956, and the Rbar ranges between 0.31 and 0.489. The chronology is considered reliable (EPS > 0.85) from 1380 AD, at which point the sample depth is nine.

(Figure 2 near here)

3.2 Correlations between the tree-ring width index and climate factors

Figure 3a shows that the tree-ring width index correlates positively and significantly with precipitation in February, and has a positive correlation with T_{mean}, T_{max}, and T_{min}, most notably with T_{mean} and T_{min}. For the 15-month period from the previous July to the current September, the tree-ring width index correlates significantly and positively with the monthly T_{min} except for that of the previous August. Correlation with annual Tmin (from the previous August through current July, Tmin87) is at the 0.01 significance level.

The first-differenced correlations between the tree-ring width index and climate data show obvious variation (Figure 3b). The tree-ring width index correlates significantly and positively with precipitation of the previous September and the current May, but negatively with precipitation of the previous December. The tree-ring width index shows clear correlations with T_{mean} and T_{min} and correlates significantly and positively with T_{min} of the previous September and November and current February, June, and July. The positive correlation with the annual T_{min} is at the 0.01 significance level.

The tree-ring width index is most strongly correlated with the annual T_{min} ($r = 0.767$, $p<0.001$). This correlation remains strong and positive after first-differencing ($r = 0.583$, $p<0.001$), which indicates that the tree-ring width index is suitable for reconstructing the annual Tmin for the given period.

(Figure 3 near here)

https://doi.org/10.5194/cp-2020-93
Preprint. Discussion started: 10 August 2020

3.3 Reconstruction development and verification

The tree-ring width index for the current year (SF_t) was selected as the predictor to reconstruct the annual mean minimum temperature departure (Tmin87):

$$\mathrm{Tmin87} = -2.497 + 2.348 SF_t . \qquad (1)$$

The variance for the entire calibration period (1960–2014) was 58.8%, adjusted to 58%. The *F* value is 74.187, which is far more than the confidence level of 0.001. The transfer function is therefore highly significant (Figure 4a and 4b).

(Figure 4 and Table 2 near here)

Cross-validation for the calibration period 1960–2014 shows that the sign test (ST) and the first difference sign test (FST) are all significant at the 0.01 level (Table 2). ST/FST are also significant for the split periods 1960–1991 and 1984–2014, indicating that the reconstructed Tmin87 is in good agreement with the instrumental values for the split periods and for the overall period. The product mean value of 5.13 ($p < 0.01$) implies favorable coincidence in the two series. A reduction error (RE) value of 0.557 for the whole 1960–2014 period indicates a high degree of similarity between the reconstructed and instrumental series. The correlation coefficient (r) of the first-differenced reconstructed and instrumental series is 0.583 ($p < 0.001$), F = 26.218 ($p < 0.001$), ST/FST ($p < 0.01$) and RE = 0.302 were all significant. Thus Eq. (1) is suitable for reconstructing changes in Tmin87.

3.4 Tmin87 change since 1380 AD

The reconstructed Tmin87 from 1380–2014 AD (Figure 4c) shows clear interannual variations in temperature. The 5 coldest years were 1488, 1490, 1824, 1862, and 1872; the 5 warmest years were 1418, 1996, 1999, 2009, and 2010. The mean of the reconstructed Tmin87 was –0.15°C (standard deviation $\sigma = 0.41$). Tmin87 values below the mean – 0.5σ are defined here as ‘cold’, and values above the mean + 0.5σ are ‘warm’. The coldest periods lasting more than 5 years were 1483–1495, 1555–1568, 1586–1602, 1686–1696, 1840–1854, 1872–1876, 1893–1901, 1910–1920, 1961–1968, and 1975–1983. Of these, 1586–1602 was the longest period and experienced the lowest temperatures, followed by 1840–1854. The warmest periods lasting more than 5 years were 1409–1424, 1504–1509, 1655–1659, 1729–1739, 1775–1779, 1781–1813, and 1991–2009. The longest warm period was 1781–1813 and the warmest interval was 1991–2009, followed by 1409–1424. Changes at both high and low frequencies over the study period clearly indicate that the climate on the TP has been warming, especially since the 1980s.

https://doi.org/10.5194/cp-2020-93
Preprint. Discussion started: 10 August 2020

Climate of the Past Discussions

3.5 Spatial representation

The correlation between the CRU gridded annual Tmin over China and the instrumental and reconstructed series for the period 1960–2014 (Figure 5) shows that the instrumental data is highly representative (Figure 5a), and correlates well with the gridded annual Tmin for most of China. The correlation is especially significant ($p < 0.1$) on the TP, the northwestern Yunnan-Guizhou Plateau, the Loess Plateau, the northern Inner Mongolia Plateau, most of the middle and lower Yangtze Plain, the North China Plain, and most of the Northeast Plain. The spatial representation of the reconstructed Tmin87 is evident in Figure 5b. The reconstructed Tmin87 also correlates significantly with the gridded Tmin87 of the TP, the northwestern Yunnan-Guizhou Plateau, the Loess Plateau, and the northern Inner Mongolia Plateau, but differs from the instrumental data. If "high correlation" is defined by a correlation coefficient > 0.6, the high-correlation zone for the reconstructed Tmin87 is discontinuous and shrunken.

(Figure 5 near here)

The first-differenced instrumental data cover a relatively small spatial area and only correlates significantly with the CRU gridded data over the TP (Figure 5c). The high spatial representation of the first-differenced reconstructed Tmin87 is mainly reflected over the TP, especially in the Animaqin Mountains (Figure 5d).

3.6 Relationship between volcanic activity and minimum temperature

A comparison of large volcanic eruption events and the reconstructed Tmin87 is shown in Figure 6. Temperature may decrease in the year of the eruption, or 1, 2, or even 3 years after the event. For strong volcanic eruptions with VEIs greater than or equal to 5, the number ratio of volcano eruption /temperature decrease in the year of the eruption or the following year is 46/35. For most years, large volcanic eruptions coincide with a drop in the Tmin across the study area.

(Figure 6 and Figure 7 near here)

Changes in Tmin change on the TP in the period 1380–2014 AD have been greatly influenced by large eruptions globally, especially in the Northern Hemisphere. Globally, Tmin decreases in the year of an eruption and one to two years thereafter (Figure 7a). For the first year following the eruption, the relationship is at 0.05 significance level. Eruptions in the Northern and Southern Hemispheres (Figure 7b and 7c) also coincide with a Tmin decrease in the year of the eruption, and for one and two years thereafter. However, eruptions in the Northern Hemisphere have a more obvious influence T_{min} in the study area, as indicated by the strong drop in temperature in the first year following an eruption (Figure 7b). Southern Hemisphere mid-latitude eruptions occur at greater distances from the TP and therefore have a correspondingly weaker influence on T_{min}.

https://doi.org/10.5194/cp-2020-93
Preprint. Discussion started: 10 August 2020

T_{min} in the study area decreases significantly in the years following volcanic activity at low latitudes (Figure 7d). Eruptions in the mid-latitudes of the Northern Hemisphere clearly coincide with drops in temperature, but the decrease is not statistically significant (Figure 7e). Eruptions in the mid-latitudes of the Southern Hemisphere and in the high latitudes of the Northern Hemisphere also coincide with reduced T_{min} in the year of the eruption and in the following year, but the decreases are not statistically significant (Figure 7f and 7g).

4 Discussion

4.1 Reliability of the Tmin reconstruction

The correlation between the tree-ring width index and climate factors shows that the relationship between tree radial growth and precipitation is not statistically significant except in February. With the thick topsoil and humid climate in spring and summer, the study area meet the needs of tree radial growth. However, according to instrumental data from the GL weather station (Table 1), which is near the sampling site, the annual T_{mean} and T_{min} are about 2.2℃ and around -7℃, respectively, and temperature is low for tree growth. The statistically significant positive correlation with temperature shows that tree radial growth in this area is restricted by temperature. As one would expect, T_{min} is the most limiting, followed by T_{mean} and T_{max}.

It should be mentioned that the CE value of the validation period remained negative for the period from 1960 to 1983 even though we tried to select different meteorological stations and different observation intervals in the analysis process. Our preliminary conclusion is that this is probably a result of a distortion of the meteorological data due to the poor management and/or the relocation of meteorological stations during the 1950s and 1960s on TP. However, the cross-validation results-indicate that the equation is reliable.

The reconstructed Tmin87 in this study was further compared with other minimum temperature reconstructions from other regions of the TP, including Hy (northeastern TP; Zhang et al., 2014), QML(ZHD) (central TP; He et al., 2014), HBL (eastern TP; Gou et al., 2007), YS (south-central TP; Liang et al., 2008), and LIT(TAN) (southeastern TP; Li and Li, 2017). As a result of differences in reconstruction factors, study regions, and methods of chronology establishment, there are some differences between the chronologies. For example, there are significant regional differences in T_{min} reconstructions over the past 100 years. However, there is also notable consistency at the interannual-multidecadal scale. The correlation coefficients between our reconstruction and each sequence are 0.227 (Hy; $p < 0.01$), 0.328 (QML(ZHD); $p < 0.01$), 0.499 (HBL; $p < 0.000$), 0.235 (YS; $p < 0.01$), 0.317 (LIT(TAN); $p < 0.01$); the closer the sequence is to the study site, the more similar the changes in T_{min} are. For example, the present Tmin87 is strongly correlated with the HBL reconstruction (Figure 8d), which is nearest

https://doi.org/10.5194/cp-2020-93
Preprint. Discussion started: 10 August 2020

to our study. Both reconstructions show low-temperature periods at the end of the 16th century and from the 1670s to the 1720s. Although it is located further from the study area, the Hy reconstruction also shows cold periods in the late 15th century, at the end of the 16th century, at the beginning of the 18th century, and in the middle of the 19th century (Figure 8a). Similarly, the low-temperature periods in the late 15th and late 16th centuries, the 1670s to 1720s, and the 1960s to 1980s are in agreement with those in the QML(ZHD) reconstruction (Figure 8b). The low-temperature interval in the 1960s–80s coincides with the cold interval in the YS reconstruction (Figure 8e). Finally, although the LIT(TAN) reconstruction is also located in another region of the TP, its low-temperature intervals are consistent with those in our reconstruction (e.g., at the end of the 15th century, 1670s–1720s, 1840s–1940s, and 1960s–80s) (Figure 8f). The consistency of these results across multiple regions of the TP are indicative of the reliability of our reconstruction.

4.2 The effect of volcanic activity on the reconstructed Tmin87

As shown in Figure 6, the cooling probability in the year of or the year following a large volcanic eruption is very high. The effects of the Tambora volcano in 1815 (VEI = 7) were recorded in many parts of the world. Our reconstruction indicates that temperatures on the TP dropped by about 0.5°C in 1816, the year following the eruption. On the southeastern TP, the cold period from 1816 to 1822 may have also been related to the Tambora eruption (Liang et al., 2008). Other research in the northeastern TP has shown that cold years can be matched with known equatorial volcanic events in 15 of 21 cases (Zhang et al., 2014). We compared years of cooling we identified in this study with those identified by Zhang (in brackets). The results are as follows: 1453(1453), 1467 and 1468 (1465, 1467, and 1468), 1602(1602), 1641 and 1644 (1641 and 1643), 1674 and 1675 (1674, 1675, and 1676), 1681(1681), 1809(1810), 1816 and 1818 (1818), 1831 and 1833 (1831 and 1833), 1971(1971), 1995(1995). It can be seen that the cooling years identified by the two studies are either the same or within a year of each other. On the southeastern TP, the 15 coldest years of the past 304 years occurred mostly within 1-2 years of a major volcanic eruption (Li et al., 2017). Nine of these 15 cooling are also seen in our study. The results of SEA analysis further confirm that the temperature of the TP is affected by strong volcanic eruptions, especially those occurring at low latitudes, and that cooling occurs in the study area within a year or two of a major eruption.

Studies have shown that the influence of low-latitude volcanic activity may be wider and more obvious than that of high-latitude activity (Cronin, 1971). Because the altitude of the troposphere is lowest at the poles, about 8–9 km above the Earth's surface, volcanic ash easily passes through the troposphere and into the stratosphere, where atmosphere is stable, so the volcanic ash cannot move widely and only influence a relatively small area. The

https://doi.org/10.5194/cp-2020-93
Preprint. Discussion started: 10 August 2020

troposphere altitude near the equator is 17–18 km, higher than that at the poles and high latitudes, the volcanic ash enters the troposphere, then as the atmosphere circulates, influences wide areas such as TP. This is one of the reasons why volcanic eruption at low latitude has obvious influence on the TP Tmin compared with volcanicity at high latitude.

The mechanisms related to how volcanic eruptions influence temperature are undoubtedly complex, and temperature variability is further driven by other factors, such as circulation patterns like ENSO (Breitenmoser et al., 2012; D'Arrigo et al., 2011; Duan et al., 2019). Cooling on the TP as a result of large volcanic eruptions may be weakened or masked by other influencing factors (Duan et al., 2018), which is likely why a one-to-one correspondence between large eruptions and cooling are not observed. Establishing a deeper understanding of the relationship between eruptions and cooling will depend on the broadening the spatial network of long-term, temperature-sensitive chronologies from the TP.

5 Conclusions

This study establishes a 667-year tree-ring width chronology for the east-central TP. The anomaly sequence of the annual Tmin (Tmin87) was reconstructed for the period 1380–2014 AD. There is clear interannual variability in Tmin during the 1380–2014 AD period. The lowest temperatures with the longest duration occurred in 1586–1602; the longest and warmest interval was 1991–2009. The Tmin on the TP has been increasing, especially since the 1980s. The SEA analysis shows that Tmin decreased in the year following strong volcanic activity at low latitudes, which had a significant influence on Tmin. Thus, the climate across the eastern central TP is sensitive to large-scale background climatic factors such as volcanic activity. Further investigations are needed to fully understand the connection between volcanic eruptions and temperature on the TP, and to incorporate this information into regional annual and decadal predictions of temperature.

Author contribution

Yong Zhang, Xuemei Shao took the tree ring samples and design this study, Yajun Wang and Yong Zhang analysed the data and prepared the manuscript, Mingqi Li prepared volcanic data and took the tree ring samples.

Acknowledgements

This study was supported by the National Key R&D Program of China [Grant No. 2016YFA0600401] and the National Natural Science Foundation of China (Grant No. 41630529 and 41430528).

References

Brad, A. J., Mann, M. E., and Ammann, C. M.: Proxy evidence for an el niño-like response to volcanic forcing., Nature, 426, 274-278, 2003.

Breitenmoser, P., Beer, J., Broennimann, S., Frank, D., Steinhilber, F., and Wanner, H.: Solar and volcanic fingerprints in tree-ring chronologies over the past 2000 years, Palaeogeogr. Palaeocl., 313-314, 127-139, 10.1016/j.palaeo.2011.10.014, 2012.

Chen, F., Zhang, Y., Shao, X. M., Li, M. Q., and Yin, Z. Y.: A 2000-year temperature reconstruction in the animaqin mountains of the tibet plateau, china, Holocene, 26, 1904-1913, 2016.

Cronin, J. F.: Recent volcanism and the stratosphere, Science, 172, 847-849, 1971.

D'Arrigo, R., Seager, R., Smerdon, J. E., LeGrande, A. N., and Cook, E. R.: The anomalous winter of 1783-1784: was the laki eruption or an analog of the 2009-2010 winter to blame? Geophys. Res. Lett., 38, L5706, 10-1029, doi:10.1029/2011GL046696, 2011.

D'Arrigo, R., Wilson, R., and Anchukaitis, K. J.: Volcanic cooling signal in tree ring temperature records for the past millennium, Journal of Geophysical Research Atmospheres, 118, 9000-9010, 2013.

Duan, J. P., Li, L., Ma, Z. G., Esper, J., Büntgen, U., Xoplaki, E., Zhang, D. J., Wang, L., Yin, H., and Luterbacher, J.: Summer cooling driven by large volcanic eruptions over the tibetan plateau, J. Climate, 31, 9869-9879, 10.1175/JCLI-D-17-0664.1, 2018.

Duan, J. P., Wu, P. L., and Ma, Z. G.: Reconciling the discrepancy of post-volcanic cooling estimated from tree-ring reconstructions and model simulations over the tibetan plateau, Atmosphere-Basel, 10, 738, 10-3390, 10.3390/atmos10120738, 2019.

Filion, L., Payette, S., Gauthier, L., and Boutin, Y.: Light rings in subarctic conifers as a dendrochronological tool, Quaternary Res., 26, 272-279, 1986.

Gou, X. H., Chen, F. H., Jacoby, G., Cook, E., Yang, M. X., Peng, J. F., and Zhang, Y.: Rapid tree growth with respect to the last 400 years in response to climate warming, northeastern tibetan plateau, Int. J. Climatol., 27, 1497-1503, 2007.

Gou, X. H., Deng, Y., Chen, F. H., Yang, M. X., Fang, K. Y., Gao, L. L., Yang, T., and Zhang, F.: Tree ring based streamflow reconstruction for the upper yellow river over the past 1234 years, Chinese Science Bulletin, 55, 4179-4186, 2010.

Gou, X. H., Peng, J. F., Chen, F. H., Yang, M. X., Levia, D. F., and Li, J. B.: A dendrochronological analysis of maximum summer half-year temperature variations over the past 700 years on the northeastern tibetan plateau, Theor. Appl. Climatol., 93, 195-206, 10.1007/s00704-007-0336-y, 2008.

https://doi.org/10.5194/cp-2020-93
Preprint. Discussion started: 10 August 2020

He, M. H., Yang, B., and Datsenko, N. M.: A six hundred-year annual minimum temperature history for the central tibetan plateau derived from tree-ring width series, Clim. Dynam., 43, 641-655, 2014.

Holmes, R. L.: Computer-assisted quality control in tree-ring dating and measurement, Tree-Ring Bull, 44, 69-75, 1983.

Jia, P. Q., and Shi, G. Y.: Study on the effects of volcanic eruption and solar activity on climate in china in recent 50 years, Plateau Meteorology, 20, 225-233, 2001.

Lamarche, V. C., and Hirschboeck, K. K.: Frost rings in trees as records of major volcanic eruptions, Nature, 307, 121-126, 1984.

Li, M. Q., Huang, L., Yin, Z. Y., and Shao, X. M.: Temperature reconstruction and volcanic eruption signal from tree-ring width and maximum latewood density over the past 304 years in the southeastern tibetan plateau, Int. J. Biometeorol., 1-12, 2017.

Li, T., and Li, J. B.: A 564-year annual minimum temperature reconstruction for the east central tibetan plateau from tree rings, Global & Planetary Change, 157, 165-173, 2017.

Liang, E. Y., Shao, X. M., and Qin, N. S.: Tree-ring based summer temperature reconstruction for the source region of the yangtze river on the tibetan plateau, Global & Planetary Change, 61, 313-320, 2008.

Liang, H. X., Lyu, L., and Wahab, M.: A 382-year reconstruction of august mean minimum temperature from tree-ring maximum latewood density on the southeastern tibetan plateau, china, Dendrochronologia, 37, 1-8, 2016.

Meko, D., and Graybill, D. A.: Tree-ring reconstruction of upper gila river discharge, Jawra Journal of the American Water Resources Association, 31, 605-616, 1995.

Melvin, T. M., and Briffa, K. R.: A “signal-free” approach to dendroclimatic standardisation, Dendrochronologia, 26, 71-86, 2008.

Michaelsen, J.: Cross-validation in statistical climate forecast models., Journal of Applied Meteorology, 26, 1589-1600, 1987.

Mitchell, T. D., and Jones, P. D.: An improved method of constructing a database of monthly climate observations and associated high‐resolution grids, Int. J. Climatol., 25, 693-712, 2005.

Robock, A.: Volcanic eruptions and climate, Rev. Geophys., 38, 191-219, 2000.

Robock, A., and Mao, J.: Winter warming from large volcanic eruptions, Geophys. Res. Lett., 19, 2405-2408, 1992.

Salzer, M. W., and Hughes, M. K.: Bristlecone pine tree rings and volcanic eruptions over the last 5000 yr, Quaternary Res., 67, 57-68, 2007.

Singh, Y. P., and Badruddin: Statistical considerations in superposed epoch analysis and its applications in space research, J. Atmos. Sol.-Terr. Phy., 68, 803-813, 10.1016/j.jastp.2006.01.007, 2006.

Tognetti, R., Lasserre, B., Battipaglia, G., Saurer, M., Cherubini, P., and Marchetti, M.: Tree-ring responses in araucaria araucana to two major eruptions of lonquimay volcano (chile), Trees, 26, 1805-1819, 2012.

Yao, T. D., Thompson, L. G., Mosbrugger, V., Zhang, F., Ma, Y. M., Luo, T. X., Xu, B. Q., Yang, X. X., Joswiak, D. R., and Wang, W. C.: Third pole environment (tpe), Environmental Development, 3, 52-64, 2012.

https://doi.org/10.5194/cp-2020-93
Preprint. Discussion started: 10 August 2020

Zhang, X. G., and Zhang, F. G.: The relationship between large volcanic eruptions and the dryness/wetness and cold/warm in china, Acta Meteorologica Sinica, 3, 196-207, 1985.

Zhang, Y., Shao, X. M., Yin, Z. Y., and Wang, Y.: Millennial minimum temperature variations in the qilian mountains, china: evidence from tree rings, Climate of the Past Discussions, 10, 341-380, 2014.

Zheng, J. Y., Bian, J. J., and Ge, Q. S.: The climate regionalization in china for 1981-2010, Chinese Science Bulletin, 58, 3088-3099, 2013.

https://doi.org/10.5194/cp-2020-93
Preprint. Discussion started: 10 August 2020

Figures and Tables

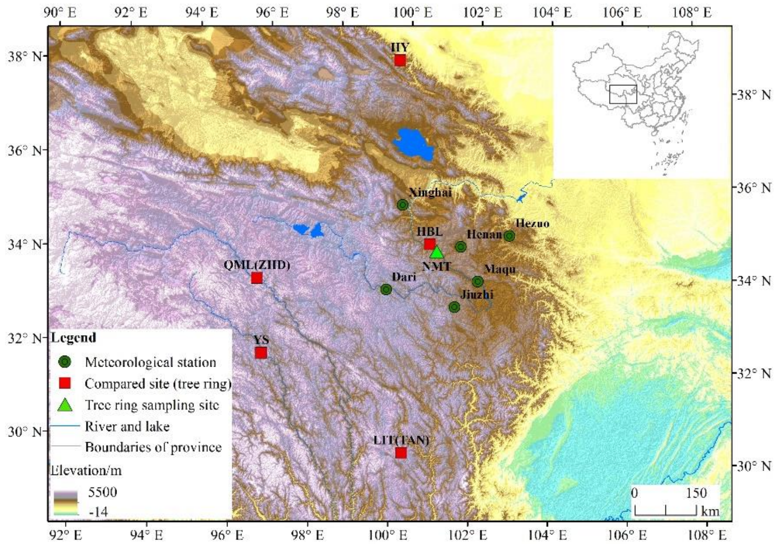

Figure 1. Locations of the Sampling site, meteorological stations, and compared sites. The data of digital elevation model is provided by Geospatial Data Cloud site, Computer Network Information Center, Chinese Academy of Sciences. (http://www.gscloud.cn)

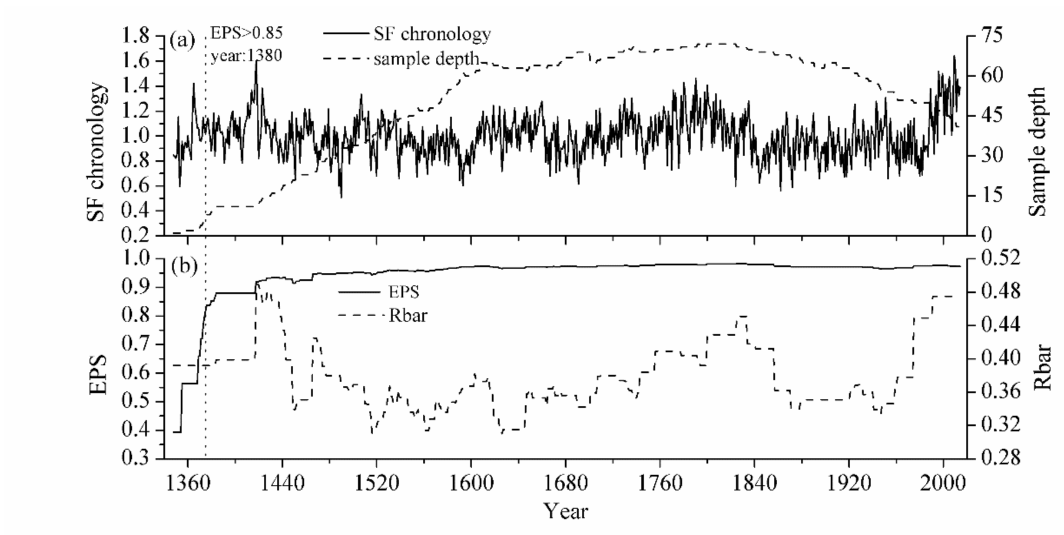

Figure 2. (a) Tree-ring width chronology; (b) EPS and Rbar values. The dotted vertical line denotes the year 1380CE, which is when the EPS value exceeds the 0.85 threshold.

https://doi.org/10.5194/cp-2020-93
Preprint. Discussion started: 10 August 2020

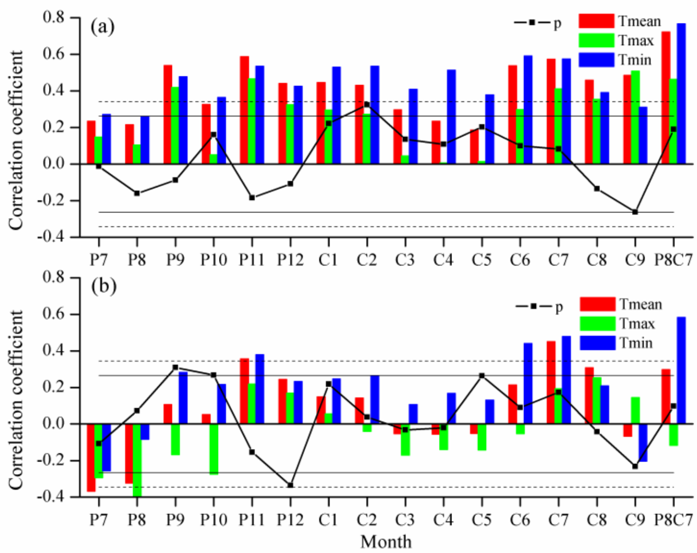

Figure 3. Correlations between (a) the tree-ring width index and climate data, and (b) the first-differenced tree-ring width index and climate data. The solid lines indicate the 0.05 significance level; the dashed lines show the 0.01 significance level. P = previous year; C = current year; P8C7 = previous August to current July

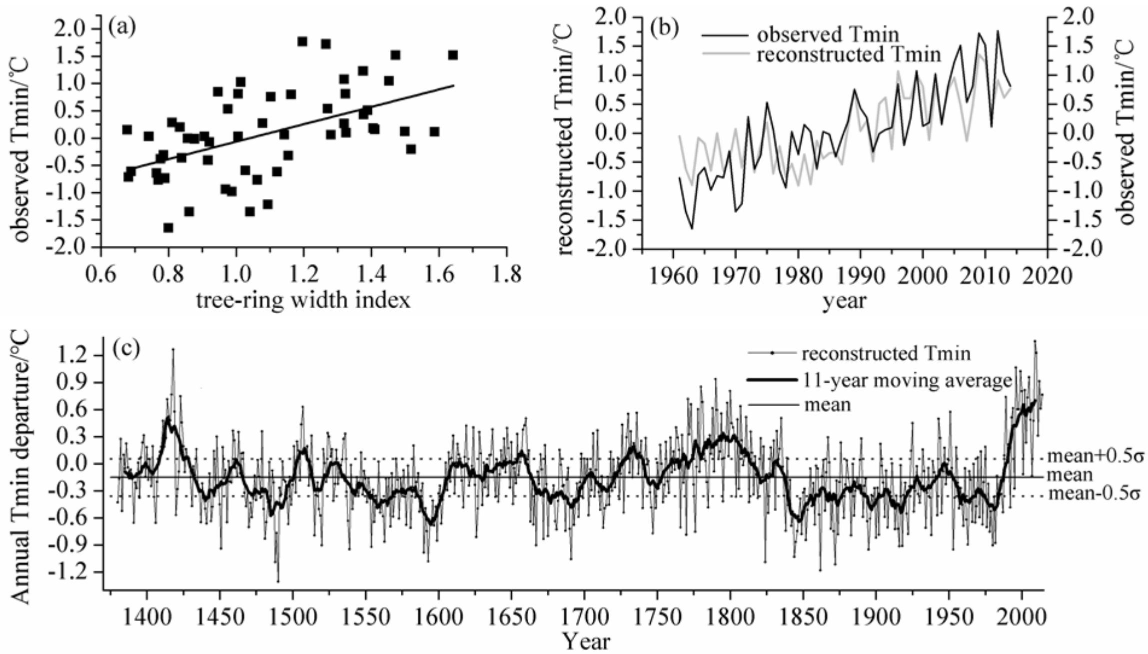

Figure 4. (a) Scatter plot of tree-ring index and instrumental annual Tmin. (b) Instrumental (black line) and reconstructed (gray line) annual Tmin. (c) Changes in annual Tmin since 1380 AD and the 11-year moving average (red line).

https://doi.org/10.5194/cp-2020-93
Preprint. Discussion started: 10 August 2020

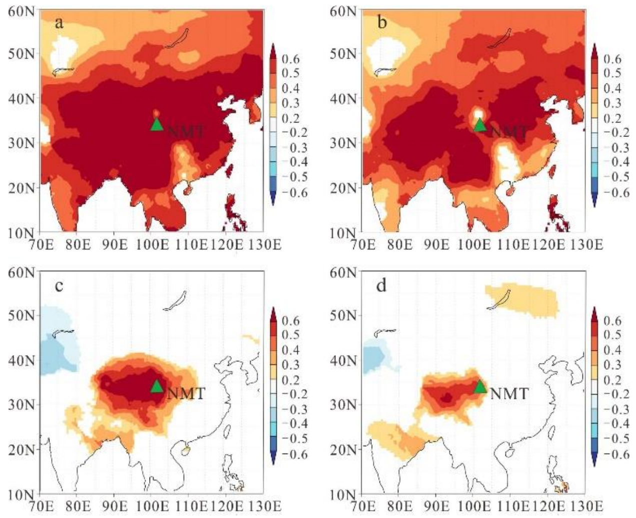

Figure 5. Correlations of CRU Tmin87 with Tmin87: (a) instrumental; (b) reconstructed; (c) first-differenced instrumental; and (d) first-differenced reconstructed

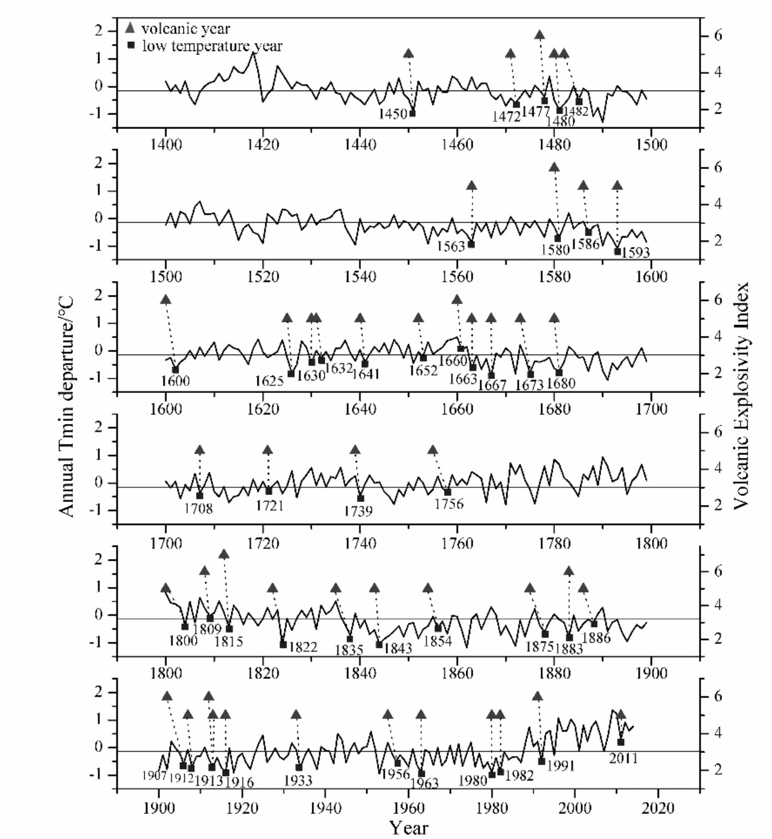

395 **Figure 6. Plot of the VEI of large volcanic eruptions (black triangle) and cold years (black square). The numbers indicate the years of the volcanic eruptions.**

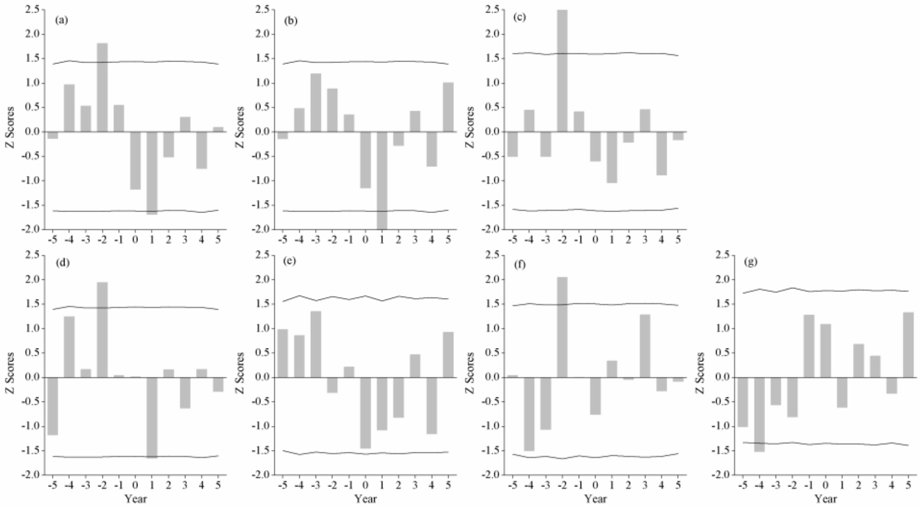

Figure 7. SEA analysis of the impact of volcanic eruptions (VEI ≥ 5) on Tmin for the period 1380–2014 AD: (a) global; (b) Northern Hemisphere; (c) Southern Hemisphere; (d) low latitudes 30°S–30°N; (e) Northern Hemisphere mid-latitude 30°N–60°N ; (f) Southern Hemisphere mid-latitude 30°S–60°S; and (g) Northern Hemisphere high latitude. 0 = year of volcanic eruption; –1 = year before eruption; 1 = year after eruption. Solid line represents the 0.05 significance level.

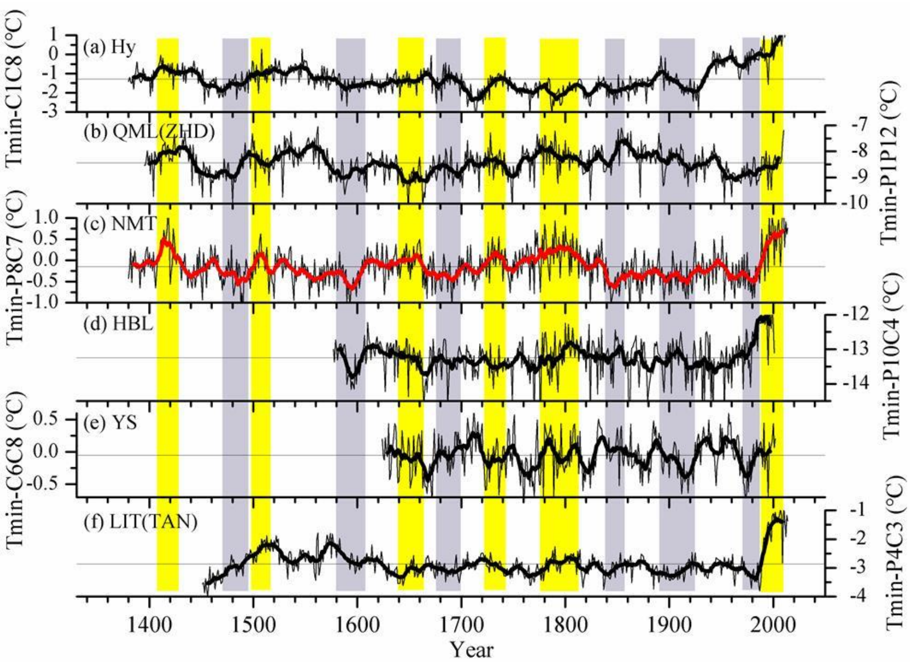

Figure 8. Comparison of our reconstructed Tmin87 with other Tmin reconstructions on the TP for the period 1380–2014 AD. (a) Hy, January-August Tmin on the northeastern TP (Zhang et al., 2014); (b) QML(ZHD), January–December Tmin on the central TP (He et al., 2014); (c) Our study; (d) HBL, October–April Tmin on the eastern TP (Gou et al., 2007); (e) YS, June–August Tmin on the south-central TP (Liang et al., 2008); (f) LIT(TAN), April-March Tmin on the southeastern TP (Li and Li, 2017). Yellow columns indicate warm periods in our reconstruction; grey columns indicate cold periods.

https://doi.org/10.5194/cp-2020-93
Preprint. Discussion started: 10 August 2020

Climate of the Past Discussions

Table 1. Meteorological station details

Station	Longitude	Latitude	Elevation (m)	Observation time span	Annual P (mm)	Annual T_{mean} (°C)	Annual T_{max} (°C)	Annual T_{min} (°C)
ZXZ	99°12′	34°16′	4211.1	1959–1997	459.1	−3.85	3.94	−10.10
DR	99°39′	33°45′	3967.5	1956–2015	551.7	−0.79	6.90	−6.88
XH	99°59′	35°35′	3323.2	1960–2015	362.8	1.44	9.80	−5.79
GL	100°15′	34°28′	3719	1991–2015	512.4	2.25	9.07	−6.76
TD	100°39′	35°16′	3289.4	1954–1998	424.2	0.51	10.00	−7.13
GN	100°45′	35°35′	3120	1999–2015	439.9	2.89	11.76	−3.81
ZK	101°28′	35°02′	3662.8	1957–1990	476.0	−2.18	6.25	−9.15
HN	101°36′	34°44′	3500	1960–2015	581.7	0.31	8.98	−6.58
JZ	101°29′	33°26′	3628.5	1959–2015	748.1	0.74	9.41	−5.71
TR	102°01′	35°31′	2491.5	1991–2015	403.5	6.52	14.0	−1.01
MQ	102°05′	34°00′	3471.4	1967–2015	600.4	1.71	9.13	−4.24
LMS	102°38′	34°05′	3362.7	1957–1988	779.9	1.21	9.00	−4.49
HZ	102°54′	35°00′	2910	1957–2015	546.2	2.55	11.08	−3.57

Note: ZXZ=Zhongxinzhan; DR=Dari; XH=Xinghai; GL=Guoluo; TD:=ongde; GN=Guinan; ZK=Zeku; HN=Henan; JZ=Jiuzhi; TR=Tongren; MQ=Maqu; LMS=Langmusi; HZ=Hezuo

Table 2. Statistics of cross-validation and split-period calibration/verification

Calibration Period	r	R^2_{adj}	F	p	Verification Period	ST/FST	PMT	RE	CE
1960–1991	0.470	0.194	8.228	0.008	1992–2014	22+**/18+**	3.651	0.743	0.017
1984–2014	0.740	0.532	35.166	0.000	1960–1983	22+**/17+*	2.945	0.677	–0.589
1960–2014	0.767	0.580	74.187	0.000	1960–2014	45+**/38+**	5.130	0.557	0.557

r = Pearson correlation coefficient; R^2_{adj} = variance after adjusting; ST/FST = sign test/first difference sign test; PMT = product-mean test; RE = reduction error; CE = coefficient of efficiency.

**p < 0.01; *p < 0.05